Clinical Oral Investigations (2023) 27:1289–1299
https://doi.org/10.1007/s00784-022-04763-9

RESEARCH

Amelogenesis imperfecta in a Chinese family resulting from a *FAM83H* variation and the effect of *FAM83H* on the secretion of enamel matrix proteins

Yongting Xie[1] · Mingmei Meng[1] · Li Cao[2] · Jiyun Yang[2] · Qizhao Ma[1] · Xiaojun Huang[1] · Yue Yu[1] · Qiyuan Yang[1] · Jing Zou[1] · Qin Du[3]

Received: 18 July 2022 / Accepted: 20 October 2022 / Published online: 1 November 2022
© The Author(s), under exclusive licence to Springer-Verlag GmbH Germany, part of Springer Nature 2022

Abstract

Objectives To investigate the variant of an amelogenesis imperfecta (AI) family and to explore the function of the *FAM83H* (family with sequence similarity 83 member H) in the enamel formation.

Materials and methods We investigated a five-generation Chinese family diagnosed with AI; clinical data was collected, whole-exome sequencing (WES) was conducted to explore the pathogenic gene and variants and Sanger sequencing was used to verify the variants. The three-dimensional protein structures of wild-type and mutant FAM83H were predicted using alpha fold 2. To study the possible regulatory function of Fam83h on amelogenesis, immunolocalization was performed to observe the expression of Fam83h protein in Sprague–Dawley rat postnatal incisors. The mRNA and protein level of amelogenin, enamelin, kallikrein-related peptidase-4 and ameloblastin were also detected after the *Fam83h* was knocked down by small interfering RNA (siRNA) in HAT-7 cells.

Results A known nonsense variant (c.973 C > T) in exon 5 of *FAM83H* gene was found in this family, causing a truncated protein (p.R325X). Immunolocalization of Fam83h in Sprague–Dawley rat postnatal incisors showed that Fam83h protein expression was detected in presecretory and secretory stages. When *Fam83h* expression was reduced by siRNA, the expression of amelogenin, enamelin, kallikrein-related peptidase-4 decreased. However, the expression of ameloblastin increased.

Conclusions *FAM83H* gene variant (c.973 C > T) causes AI. *FAM83H* regulates the secretion of enamel matrix proteins and affects ameloblast differentiation.

Clinical relevance This study provided that *FAM83H* variants could influence enamel formation and provided new insights into the pathogenesis of AI.

Keywords Amelogenesis imperfecta · *FAM83H* · Small interfering RNA · Enamel matrix proteins · HAT-7

Yongting Xie and Mingmei Meng equally contributed to this article and should be regarded as co-first authors.

The two correspondence authors contribute equally to this work.

✉ Jing Zou
zoujing@scu.edu.cn

✉ Qin Du
duqin@med.uestc.edu.cn

[1] State Key Laboratory of Oral Diseases & National Clinical Research Center for Oral Diseases, Department of Pediatric Dentistry, West China Hospital of Stomatology, Sichuan University, Chengdu, Sichuan, China

[2] The Sichuan Provincial Key Laboratory for Human Disease Gene Study, Centre for Medical Genetics, Sichuan Academy of Medical Sciences & Sichuan Provincial People's Hospital, University of Electronic Science and Technology, Chengdu, Sichuan, China

[3] Department of Stomatology, Sichuan Provincial People's Hospital, University of Electronic Science and Technology of China, Chengdu, Sichuan, China

Introduction

Tooth development is a highly orchestrated process that is regulated by many factors. Precise signalling pathways that form epithelial and mesenchymal cells are required for each tooth to initiate and continue along its developmental path [1]. Enamel is far more mineralized than other tooth structures and serves to protect the dentin and pulp [2]. Mature enamel is a tissue that consists of high-grade crystallites and contains no collagen or cells, so it cannot be remodelled [3]. The development of enamel can be divided into four stages: the presecretory, secretory, transition and maturation stages [4]. During the secretory stage, ameloblasts are highly polarized. These cells synthesize and secrete a limited number of structural enamel matrix proteins, most notably amelogenin (AMELX), ameloblastin (AMBN) and enamelin (ENAM), and the proteinase is matrix metalloproteinase-20 (MMP20) [5]. AMELX comprises approximately 80–90% of the organic matter within the secretory stage enamel matrix, and AMBN and ENAM comprise approximately 5% and 3–5%, respectively. MMP20 is present in trace amounts [6]. It is during the maturation stage that ameloblasts actively secrete kallikrein-related peptidase-4 (KLK4) to help remove the mass of previously secreted and partially hydrolysed matrix proteins from the enamel layer. This allows the rod and interrod crystallites to expand in volume to occupy as much space as possible within the enamel layer [4, 7, 8]. Enamel matrix proteins are necessary for proper enamel formation, but they are later reabsorbed by ameloblasts. These proteins are necessary to form enamel, but they are not part of the final maturation product [9].

Amelogenesis imperfecta (AI) is a clinically and genetically heterogeneous group of inherited conditions typically characterized by enamel defects of both primary and permanent dentitions occurring occasionally in conjunction with other dental, oral and extraoral abnormalities [10]. AI not only affects patients' masticatory function and maxillofacial appearance but also affects their psychological state. Three main AI phenotypes are generically categorized to delineate the spectrum of enamel defects, hypoplastic AI, hypomaturation AI and hypocalcified AI [11]. In the hypoplasia type, the glaze matrix forms defects in the secretory stage, which leads to the glaze matrix not reaching normal thickness or even being completely missing. Hypomaturation AI is mainly caused when the enamel matrix proteins cannot be completely removed. The enamel thickness is basically normal. However, the hardness is insufficient, and it is easy to wear. Most of the enamel shows colour change (yellow brown or brown). The hypocalcified type is the most frequent and severe type of AI. It is characterized by cheesy soft and malformed enamel, which is fragile and easily lost soon after tooth eruption [12].

Many genes are known to cause AI, and these can be inherited in an autosomal recessive, dominant or X-linked manner [13]. At present, pathogenic variants in 18 genes (*LAMB3* #150,310, *AMTN* #610,912, *ENAM* #606,585, *FAM83H* #611,927, *DLX3* #600,525, *ITGB6* #147,558, *AMBN* #601,259, *ENAM* #606,585, *ODAPH* #614,829, *RELT* #611,211, *MMP20* #604,629, *GPR68* #601,404, *SLC24A4* #609,840, *WDR72* #613,214, *FAM20A* #611,062, *ACP4* #606,362, *KLK4* #603,767, *AI1E2* #301,201, *AI1E2* #301,201) were identified to cause different phenotypes of AI according to the OMIO database (www.omio.org). *FAM83H* (family with sequence similarity 83 member H) accounts for the most AI cases and is the main causative gene in autosomal dominant hypocalcified AI. *FAM83H* functions in many cells throughout the body, but the ameloblast lineage is more sensitive than other cell types to *FAM83H* variants. Many studies have reported that *FAM83H* variants lead to AI, implying a correlation between *FAM83H* and AI [14–22].

Although many *FAM83H* variants associated with AI have been reported, the function of *FAM83H* in enamel formation and its pathogenic mechanism have not been fully elucidated. Kim et al. reported that Fam83h is highly expressed in the presecretory and secretory ameloblasts and plays an important role during enamel formation [23]. Later, some studies showed that *Fam83h* is not necessary for proper dental enamel formation in mice [24, 25], but another research showed controversial dental phenotypes, and the result did not support the notion that *Fam83h* is not necessary for proper dental enamel formation [26]. Since *FAM83H* mutation results in malformation of the enamel, we want to observe the effect of *Fam83h* on enamel matrix proteins and differentiation of ameloblasts directly.

Here, we investigated the case of a five-generation Chinese family diagnosed with AI using whole-exome sequencing, Sanger sequencing and clinical examination. We reported a known nonsense variant (c.973 C>T) in exon 5 of the *FAM83H* gene [10, 18, 23, 27] that causes a truncated protein (p.R325X) in this new Chinese family. To explore the function of *Fam83h* in enamel formation and the differentiation of ameloblasts, the distribution of Fam83h in Sprague−Dawley rat postnatal incisors was detected by immunohistochemistry of tissue sections, the expression of *Fam83h* in the odontogenic epithelial cell line HAT-7 was knocked down by small interfering RNA (siRNA) and changes in enamel matrix proteins were observed.

Materials and methods

Subjects

A Chinese family with AI was investigated in this study. This study was approved by the Ethics Committee of the Sichuan Academy of Medical Sciences-Sichuan Provincial People's Hospital (Chengdu, China). Written informed consent was obtained from all participants or their guardians. Phenotypic characterization and pedigree construction were conducted

through medical history taking and clinical and radiographic examinations. Peripheral blood samples were obtained from participants (two affected individuals V:4, III:13 and one nonaffected individual V:5) (Fig. 1i).

Variant analyses

Genomic DNA was isolated from peripheral blood using the TIANGEN Blood DNA Kit (TIANGEN, Beijing, China) in accordance with the standard protocol. We performed whole-exome sequencing (WES) of genomic DNA from three individuals (two affected individuals V:4; III:13 and one nonaffected individual V:5) via iGeneTech (Beijing, China). Analysis of WES data and annotation of variants were carried out as previously reported [28]. Polymerase chain reaction (PCR) primers for candidate genes were designed using Primer-BLAST (https://www.ncbi.nlm.nih.gov/tools/primer-blast). PCR products were analysed by agarose gel electrophoresis and were sequenced by Sanger sequencing to confirm co-segregation in all family members. Sequence variants were called by comparing the resulting sequencing data with human reference sequence and annotated with NM_198488.5 for numbering cDNA and gDNA positions, respectively.

Protein structural prediction

The three-dimensional (3D) protein structure prediction of wild-type and mutant FAM83H was predicted using alpha fold 2.

Animals and tissue preparation

The animal experimental protocol was approved by the Ethics Committee of West China College of Stomatology, Sichuan University, Chengdu, China. Rats were anaesthetized by isoflurane inhalation. They were euthanized by decapitation after anaesthesia at the 30th postnatal days for immunohistochemical staining. These tissues were then fixed in freshly prepared 4% paraformaldehyde for 24 h at 4˚C and decalcified by soaking in 10% ethylene diamine tetraaceticacid (EDTA) in phosphate buffered saline (PBS) for 30 days. Afterwards, fully decalcified samples were dehydrated in a graded ethanol series and embedded in paraffin. Paraffin Sect. (5 µm thick) were mounted on poly-L-Lysine-coated glass slides (Sigma-Aldrich).

Immunohistochemistry (IHC)

Tooth germs (incisors), sectioned as described above, were incubated with rabbit polyclonal anti-Fam83h antibody

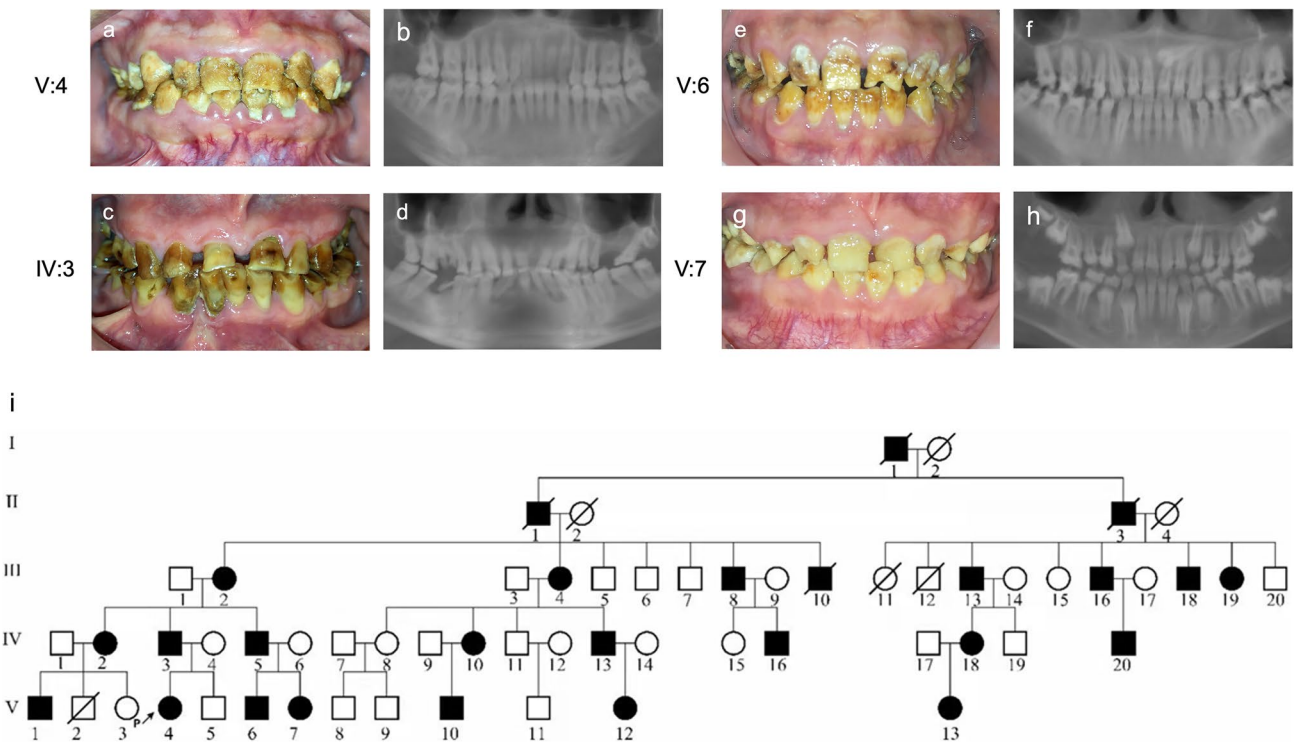

Fig. 1 Clinical phenotypes and pedigree of the family. **a, b** Frontal clinical photo and panoramic radiograph of the proband (V:4). **c, d** Frontal clinical photo and panoramic radiograph of the proband's father (IV:3). **e, f** Frontal clinical photo and panoramic radiograph of the proband's cousin (V:6). **g, h** Frontal clinical photo and panoramic radiograph of the proband's cousin (V:7). The V:6 and V:7 are brother and sister. **i** Pedigree of the family. Males are marked as squares and females as circles. An arrow indicates the proband (V:4), and the black symbols indicate the affected individuals

(rabbit polyclonal, 1.25 μg/ml, catalog number: ER1908-67 in HUABIO, China). IHC was performed following the manual of the immunohistochemical assay kit (Zhongshan Jinqiao Biological Technology Co., Beijing, China) (SP method). The sections were developed with diaminobenzidine tetrahydrochloride (DAB).

Cell culture and transfection with small interfering RNA (siRNA)

HAT-7 cell line was graciously provided by Professor Hidemitsu Harada, Department of Oral Anatomy and Developmental Biology, Osaka University Graduate School of Dentistry, Osaka, Japan. HAT-7 cells were an immortalized dental epithelial cell line derived from the cervical stem call population of 6-day-old rat mandibular incisors [29].The HAT-7 cells were plated with Dulbecco's modified Eagle's medium/F-12 (DMEM/F-12; Gibco-BRL, Grand Island, NY, USA) supplemented with 10% foetal bovine serum (Gibco-BRL, Grand Island, NY, USA) and 1% penicillin–streptomycin (Gibco-BRL, Grand Island, NY, USA). The cells were grown in a humidified atmosphere at 37 ℃ with 5% CO_2, and the medium was changed every 3 days. The cells were cultured in medium without antibiotics 24 h prior to transfection. Three different nucleotides (*Fam83h* siRNA 1, 2 and 3) targeting rat *Fam83h* mRNA (GenePharma, Shanghai, China) were designed and tested for silencing. Cells were cultured without siRNA and transfection reagent in control group, while cells were cultured only with transfection reagent in mock group. Non-silencing siRNA with no homology to any known mammalian gene was used as a negative control. Their sequences are shown in Table 1. The cells were transfected with the siRNA (50 nM) and EndoFectin™-Max transfection reagent (GeneCopoeia, Guangzhou, China) (1:1 v/v). The RNAi-mediated knockdown of *Fam83h* expression was verified by quantitative reverse transcription-polymerase chain reaction (RT-qPCR) and western blot analysis.

RNA isolation and RT-qPCR analysis

Forty-eight hours after transfection, total RNA was isolated using TRIzol reagent (CWbio, Nanjing, China), and then reversed transcribed into cDNA using the PrimeScript™ RT reagent Kit (Takara, Dalian, China). After cDNA synthesis, a real-time PCR was carried out via ABI7300 real-time PCR System (Applied Biosystems, Inc, USA) using TB Green Premix Ex Taq™II (Takara, Dalian, China). Each cycle consisted of denaturation for 30 s at 94 °C, annealing for 30 s at 59 °C and extension for 30 s at 72 °C. The sequences of the gene-specific primers are listed in Table 2. Experiments were performed in triplicate.

Western blotting analysis

Seventy-two hours after transfection, total cellular proteins were harvested with RIPA (Beyotime Biotechnology, China).

Table 1 Sequences of negative control nucleotides and the 3 different nucleotides (*Fam83h* siRNA 1, 2, 3) targeting rat *Fam83h* mRNA expression

Nucleotide	Sequence (5′→3′)
Negative control	
Sense strand	UUCUCCGAACGUGUCACGUTT
Antisense strand	ACGUGACACGUUCGGAGAATT
siRNA 1	
Sense strand	CCACCUCACUACAAAGAAUTT
Antisense strand	AUUCUUUGUAGUGAGGUGGTT
siRNA 2	
Sense strand	GCGGUAGUUAUAGCUUCAUTT
Antisense strand	AUGAAGCUAUAACUACCGCTT
siRNA 3	
Sense strand	CGGAGCUACUGGAGAAAUATT
Antisense strand	UAUUUCUCCAGUAGCUCCGTT

Cell lysates were collected from HAT-7 cells to screen the effective siRNA and to evaluate the effects of siRNA on the protein expression of Fam83h, Amelx, Ambn and Klk4. The sample were boiled in Laemmli sample buffer and loaded onto a sodium dodecyl sulfate–polyacrylamide gel (SDS-PAGE) followed by transfer onto nitrocellulose membranes. The primary antibodies were used anti-Fam83h (rabbit polyclonal, 1.25 μg/ml, catalog number: ER1908-67 in HUABIO, China), rabbit polyclonal anti-Amelx (mouse polyclonal, 2 μg/ml, catalog number: sc-365284 in SANTA, USA), rabbit polyclonal anti-Ambn (rabbit polyclonal, 2 μg/ml, catalog number: bs-12467R in Bioss, China) and mouse polyclonal anti-Klk4 (rabbit polyclonal, 2 μg/ml, catalog number: bs-1965R in Bioss, China) antibodies. Rabbit monoclonal Anti-β-actin (rabbit polyclonal, 1 μg/ml, catalog number: 49366–1 in SAB, USA) antibody was used as an internal standard.

Statistical analyses

Data were expressed as the mean ± standard deviation (SD). Statistical significance between two groups was determined using the independent samples *t* test. A P value < 0.05 was considered statistically significant. *P < 0.05, **P < 0.01, ***P < 0.001 and ****P < 0.0001. Statistical testing was performed with SPSS software (version 20.0, IBM, Armonk, NY).

Results

Clinical phenotype and variant analysis

We identified a five-generation Chinese family with AI phenotype when the proband (V:4, Fig. 1i), a 27-year-old female, presented to the Sichuan Academy of Medical

Table 2 Oligonucleotide primer sequences utilized in RT-qPCR

Gene name	Primer sequence (5′→3′)	Product size (bp)
Fam83h	F: TGCACCACGTGGATTTCCTG	131
	R: ACCGCTCATCACTACAGCAC	
Ambn	F: GAGAAAGGAGAGGGTCCA GAAG	126
	R: GTCATTGGGGAAAGCAAGAAGT	
Amelx	F: ACCTCTGCCTCCACTGTTCTC	102
	R: ACTTCTTCCCGCTTGGTCTT	
Enam	F: GGTGTCTTCCCTCTCCCTAAA	141
	R: AGTGGTTTGCCATTGTCTTTCT	
Klk4	F: CCGAACTACAATGACCCTTCTT	209
	R: TCAGATGCTACCGAGAGATTCA	

Fam83h family with sequence similarity 83 member H, *Ambn* ameloblastin, *Amelx* amelogenin, *Enam* enamelin, *Klk4* kallikrein-related peptidase-4.

Sciences-Sichuan Provincial People's Hospital (Chengdu, China) with complaints of unsightly teeth. Her pedigree contained 59 family members, 26 of whom were affected by AI according to our research. Clinical examination of affected individuals revealed that the different severity of enamel defected affected the deciduous and permanent teeth. No symptoms were observed in the individuals, other than the dental phenotype.

The proband (V:4) inherited enamel defects from her father. The teeth of the proband exhibited yellowish colouration and rough surfaces with plaque accumulation. The enamel had obvious attrition, exposing dentin (Fig. 1a). The panoramic radiograph of the proband showed that the enamel density was reduced and could not be distinguished from dentin (Fig. 1b). Clinical examination of proband's father (IV:3) showed similar clinical symptoms (Fig. 1c). Besides these symptoms, clinical features of proband's cousin (V:7) included anterior cross bite (Fig. 1g).

To identify the pathogenic variant causing the disease, we performed WES using genomic DNA from the affected family members V:4 and III:13 and the control V:5. Combined with the genetic model and the disease situation of the three people, the candidate variants in these Chinese family were screened out (Table 3). Moreover, a previously reported nonsense variant (c.973C > T) in *FAM83H* (NM_198488) is identified as causing a truncated protein at amino acid position 973.✗

V:4 and III: 13 are affected individuals, and V:5 was nonaffected individuals. "✓"indicates the site was carried, and "✗" indicates the site was not carried. *FAM83H* family with sequence similarity 83 member H; *FAM20A* FAM20A golgi associated secretory pathway pseudokinase; *LAMB3* laminin subunit beta 3.

Primer 5 was used to design primers for the variant site of the pathogenic gene. PCR amplification and Sanger sequencing were performed on DNA samples from 16 members of the family, including the proband (V:4). Nine patients carried a heterozygous variant of c.973C > T (p. R325X) in *FAM83H* gene, while seven healthy family members did not carry this variant. The results showed that the variant c.973C > T (p. R325X) of *FAM83H* gene in this family was consistent with genotype and phenotype co-segregation (Fig. 2a).

Alpha fold 2 indicated that the *FAM83H* c.973C > T variant changed the structure of protein, causing the loss of portions of the alpha-helix and random coil structure (Fig. 2b, c). The *FAM83H* disease-causing variants reported until now, including 30 nonsense mutations, 4 frameshift mutations and 2 missense mutations, were shown in Fig. 2d and Supplementary Table 1.

The expression of Fam83h in rat postnatal incisors

The result concerning the immunolocalization of Fam83h in the Sprague–Dawley rat incisors was shown in Fig. 3. The morphology of ameloblasts differed as they went into different stage. The secretory ameloblasts were highly polarized while ameloblasts in the maturation stage was shorter. Positive staining of Fam83h was found in cervical loop and pre-ameloblasts. The staining increased at the presecretory and secretory stages. No primary antibody was applied in the negative controls (Supplemental Fig. 1).

Fam83h silencing in HAT-7 cells

For the analysis of molecular function, *Fam83h* was knocked down in HAT-7 cells. RT-qPCR and western blots analysis revealed that *Fam83h* was successfully knocked down using three different siRNA and siRNA 2 showed the highest inhibition efficiency (Fig. 4a, b).

Table 3 Candidate variants in Chinese family

	Transcription	Nucleotide	Homozygote/ Heterozygote	Gnomad	V:4	III:13	V:5
FAM83H	NM_198488	c.G2363A	Heterozygote	0.0305	✓	✗	✗
FAM83H	NM_198488	c.C973T	Heterozygote	0	✓	✓	✗
FAM20A	NM_017565	c.C1206T	Heterozygote	0.002	✓	✗	✗
LAMB3	NM_001017402	c.G1149A	Heterozygote	0.0602	✓	✗	✗

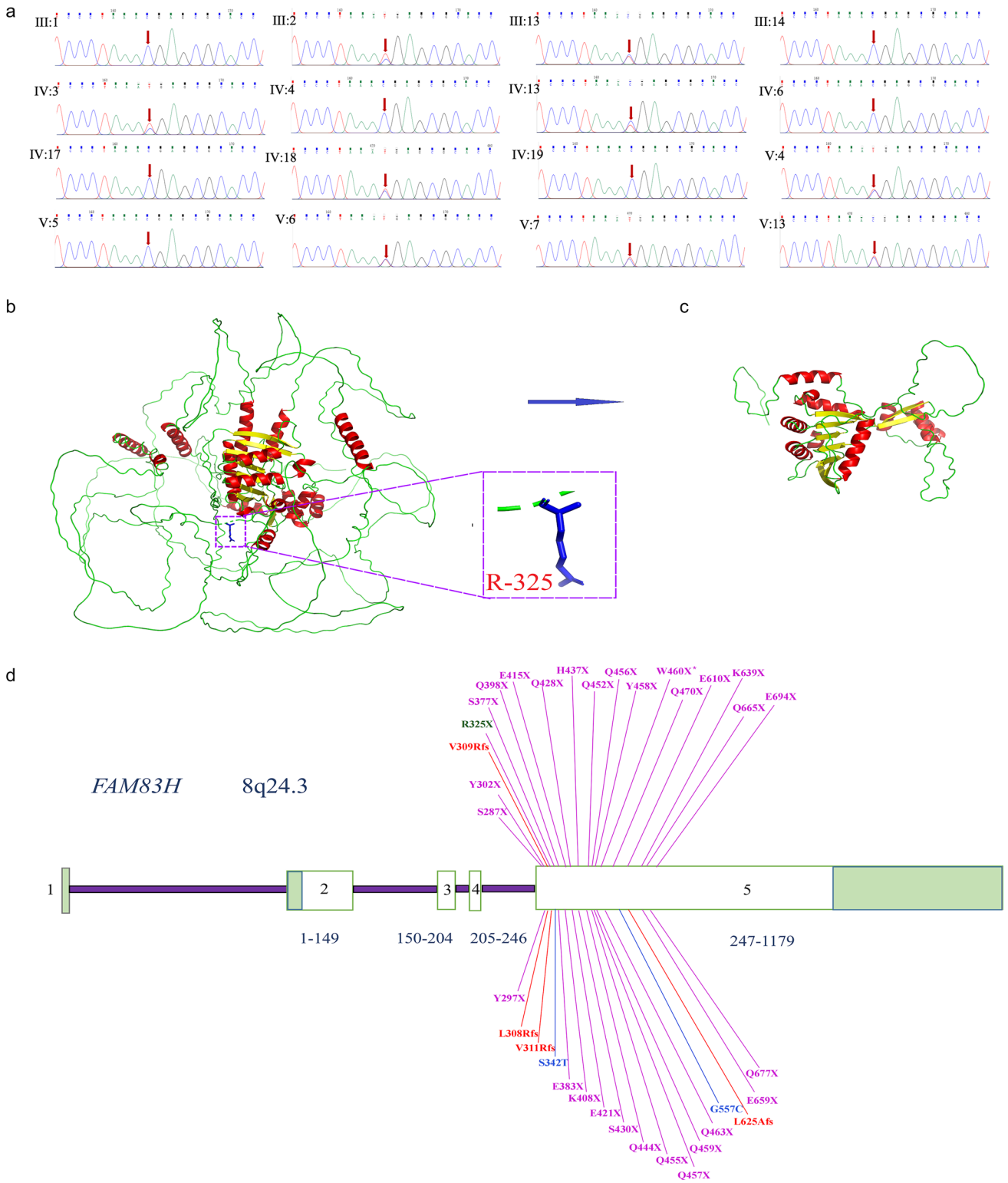

Fam83h affects HAT-7 cell differentiation

Silenced by siRNA 2, the expression of enamel matrix proteins was evaluated by RT-qPCR and western blots analysis. When *Fam83h* expression was reduced, the expression of *Enam*, *Amelx* and *Klk4* decreased and the expression of *Ambn* increased by RT-qPCR (Fig. 4c). Western blot analysis showed a decrease in Amelx and Klk4, while the expression of Ambn increased (Fig. 4d). *Fam83h* regulates the secretion of enamel matrix proteins and affects ameloblast differentiation.

◂**Fig. 2** Sanger sequencing, protein structure and *FAM83H* disease-causing variants. **a** Sanger sequencing about 16 members of this family. Proband (V:4) and other affected individuals (III:2, III:13, IV:3, IV:13, IV:18; V:6, V:7 and V:13) carried a heterozygous variant of c.973C > T (p. R325X) in *FAM83H* gene (indicated by red arrow), while nonaffected individuals (III:1, III:14, IV:4, IV:6, IV:17, IV:19 and V:5) did not carry this variant. **b** Protein structure of wild-type predicted by alpha fold 2. R-325 in the predicted model was highlighted in blue. **c** Protein structure of mutant-type predicted by alpha fold 2. **d** *FAM83H* disease-causing variants. *FAM83H* gene structure: numbered boxes indicate exons; introns are lines connecting the exons. The numbers show the range of amino acids. Shaded exon regions are non-coding regions. The 30 reported *FAM83H* nonsense mutations, 4 frameshift mutations and 2 missense mutations are labelled. The variant of c.973C > T (p. R325X) in *FAM83H* gene was highlighted in green

Discussion

AI is a heterogeneous group of genetic conditions characterized by defective enamel. The prevalence of AI is between 1/700 and 1/14000 individuals globally [30]. It is affected by many factors, and the clinical manifestations vary greatly. The treatment goal of AI always aims at protecting the oral and maxillary systems and repairing hard tissues. Until now, the ultimate treatment consists largely of full-coverage repairs or adhesive restorations. In this study, we investigated the case of a five-generation Chinese family diagnosed with AI using whole-exome sequencing, Sanger sequencing and clinical examination. We found a known nonsense variant (c.973 C > T) in exon 5 of the *FAM83H* gene that causes a truncated protein (p.R325X) in this Chinese family. Clinical examination showed that the teeth of the proband (V:4) exhibited yellowish colouration and rough surfaces with plaque accumulation. Enamel attrition was obvious, and exposed dentin was seen in each individual of this family. This variant has been reported four times before and is the most frequently reported variants in east Asia (Supplementary Table 1). These findings suggest that it may be a hot spot in east Asia. There may be a founder effect, since all the families are from east Asia. However, further investigation is needed. Interestingly, in a pair of siblings in this family, the sister manifested anterior cross bite, but the brother did not.

The human *FAM83H* gene is located at chromosome 8q24.3 and encodes an intracellular protein containing 1179 amino acids with five exons [12]. To date, 36 variants of *FAM83H* have been found to cause AI, including 30 nonsense mutations, 4 frameshift mutations and 2 missense mutations (Fig. 2d and Supplementary Table 1) [5]. In this study, alpha fold 2 indicated that the *FAM83H* c.973C > T variant changed the structure of the protein, causing the loss of portions of the alpha-helix and random coil structure, as previously reported [18].

In this study, immunolocalization of Fam83h in Sprague–Dawley rat postnatal incisors showed that Fam83h protein expression was detectable in preameloblasts and ameloblasts, and the staining increased at the presecretory and secretory stages, which is consistent with Kim et al.'s study [23]. The detection of Fam83h in the presecretory and

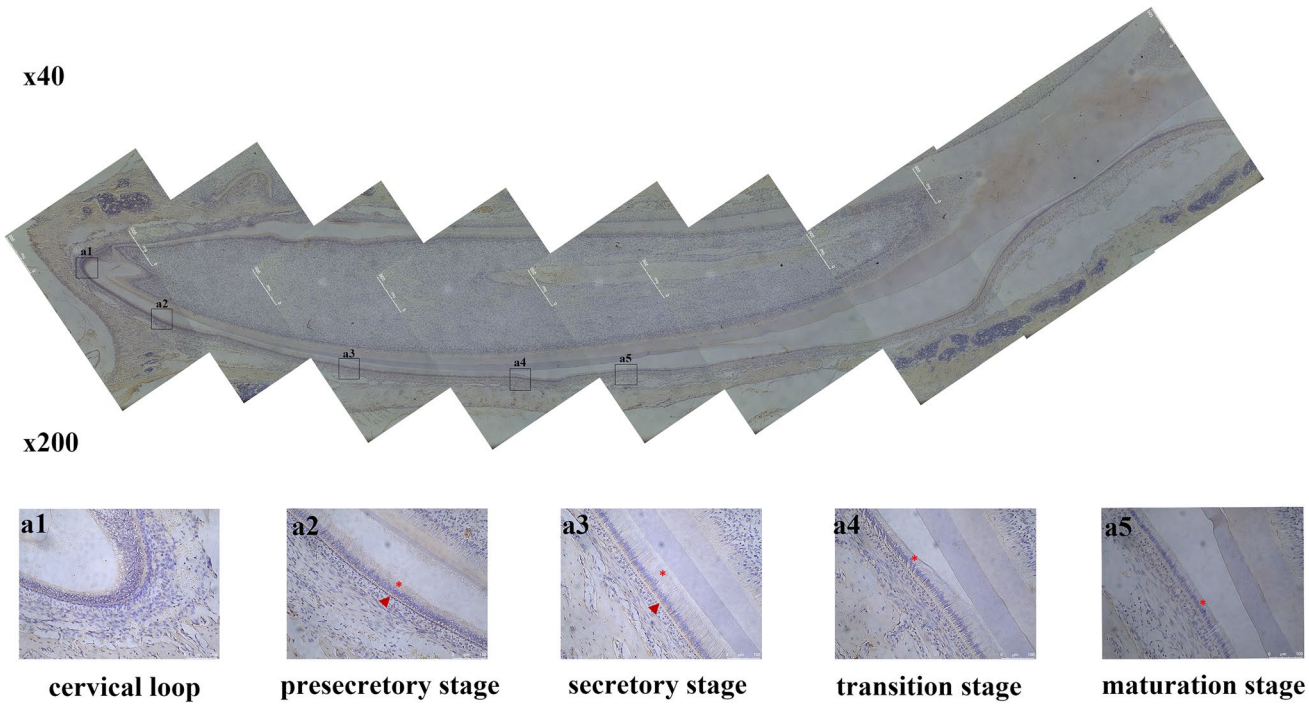

Fig. 3 Localization of Fam83h in incisors of postnatal rat. Fam83h protein expression was detected in cervical loop and ameloblasts at different stage. The staining increased at the presecretory and secretory stages

secretory ameloblasts indicates that it may play an important role in these two stages of enamel formation. The anatomy of ameloblasts changes quickly and dramatically from the secretory to maturation stage. Ameloblasts acquire distinctive properties and generate a synthetic protein apparatus to secrete the organic enamel matrix in the presecretory stage. During the secretory stage, ameloblasts secrete the entire enamel thickness [31]. Throughout the maturation stage, organic materials and water are removed, and the enamel is converted into the hardest tissue in the human body by continuous deposition of phosphate and calcium [32, 33]. In addition, defects in the *FAM83H* gene are mostly frequently reported in autosomal-dominant hypocalcified AI (ADHCAI) cases. ADHCAI occurs during the maturation stage and is characterized by insufficient transport of calcium ions into the developing enamel. However, the expression of Fam83h increased during the presecretory and secretory stages in previous studies and in this study. We speculated that Fam83h may play an important role in the presecretory and secretory stages of enamel formation, while ADHCAI may play a role in the maturation stage. This may require further investigation.

Although many *FAM83H* variants associated with AI have been reported, the function of *FAM83H* in enamel formation and its pathogenic mechanism have not been fully elucidated. In recent studies, it has been revealed that FAM83H colocalizes with casein kinase I (CK-1) and keratin filaments and is involved in enamel formation as a scaffold protein [24]. Kuga et al. suggested that *FAM83H* variants cause keratin disorganization and disruption of desmosomes in ameloblasts [34]. Moreover, they may play a role in intercellular vesicle trafficking [35]. Further studies showed that if the heterodimer of truncated and wild-type FAM83H is transported into the nucleus, it could lower the concentration of wild-type cytosolic FAM83H below what is required for normal function [9, 27, 31]. Nevertheless, despite all these findings, the functions of *FAM83H* and the mechanisms affected by *FAM83H* variants remain elusive.

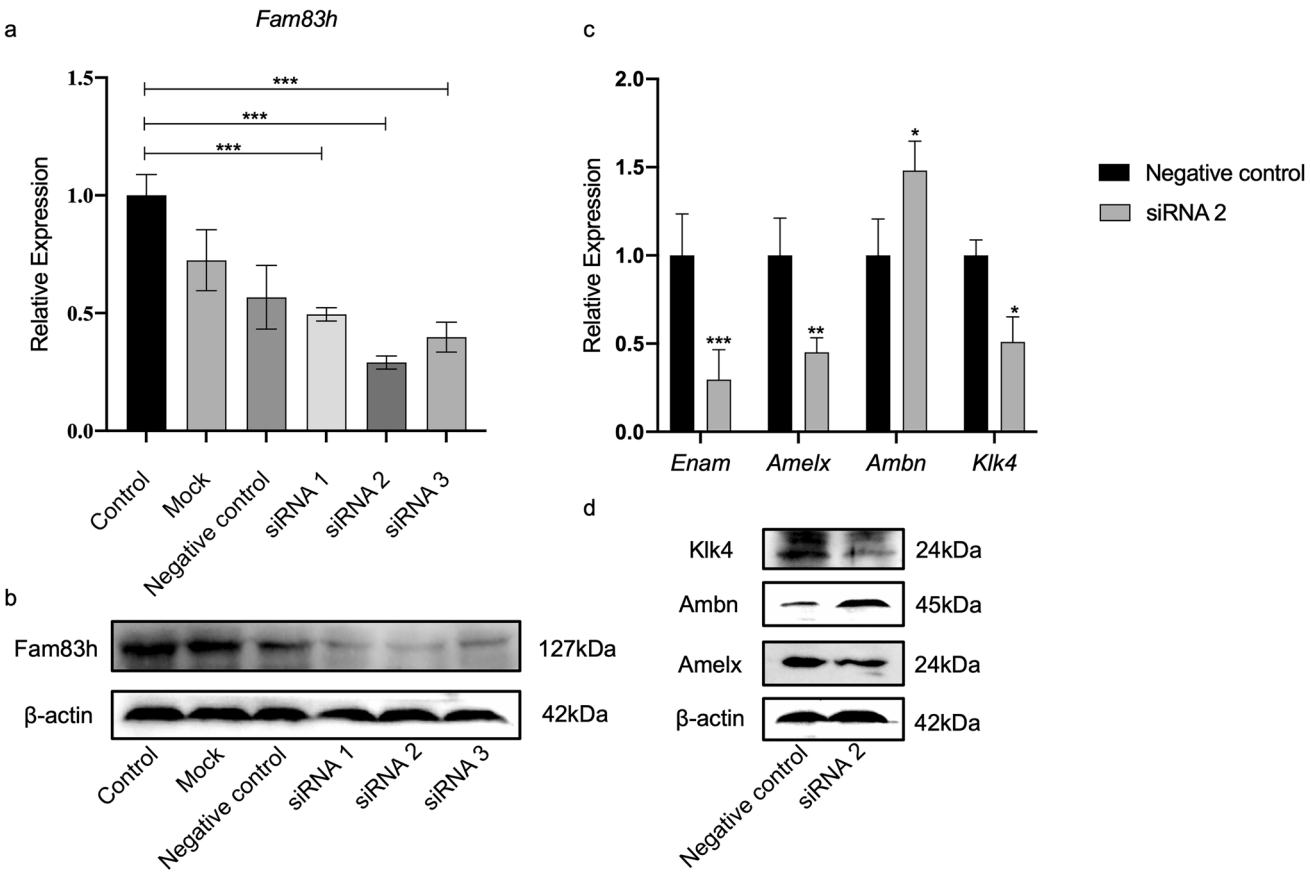

Fig. 4 *Fam83h* silencing in HAT-7 cells and the expression of enamel matrix proteins. **a, b** RT-qPCR and western blot analysis revealed that *Fam83h* was successfully knocked down by siRNA. siRNA 2 showed the highest inhibition efficiency. **c** The expression of enamel matrix proteins was evaluated by RT-qPCR. *Fam83h* was downregulated the expression of *Enam*, *Amelx* and *Klk4* while the expression of *Ambn* increased. **d** The expression of enamel matrix proteins was evaluated by western blot analysis. Fam83h was downregulated the expression of Amelx and Klk4, while the expression of Ambn increased. $^{*}P<0.05$, $^{**}P<0.01$, $^{***}P<0.001$ and $^{****}P<0.0001$

Some studies supported the conclusion that *Fam83h* is not necessary for proper dental enamel formation in mice but may act as a scaffold protein that localizes CK1. Their results showed that $Fam83h^{-/-}$ mice showed no enamel phenotype, and $Fam83h^{Tr/Tr}$ (p.Tyr297*) mice displayed obvious enamel malformation [24, 25]. This variant protein causes a disease phenotype by interfering with the normal functions of the wild-type protein expressed from the unmutated allele. Recently, a study found that outbred stock homozygous $Fam83h^{KO/KO}$ mice showed controversial dental phenotypes. The dental anomalies were seen among three homozygous $Fam83h^{KO/KO}$ mice over four generations. These phenotypes imitate the AI phenotypes [26]. This result did not support the notion that *Fam83h* is not necessary for proper dental enamel formation. Our study found that *Fam83h* could regulate the secretion of enamel matrix proteins and affect ameloblast differentiation, suggesting that *Fam83h* may play a role in enamel formation.

To explore the function of *Fam83h* in the enamel formation and differentiation of ameloblasts, the expression of *Fam83h* in odontogenic epithelial cell line HAT-7 cells was knocked down by siRNA. The changes in enamel matrix proteins were observed in this study. When *Fam83h* expression was reduced, the expression of *Enam*, *Amelx* and *Klk4* decreased, and the expression of *Ambn* increased, as shown by RT-qPCR. Western blot analysis showed a decrease in Amelx and Klk4, and the expression of Ambn increased. There were no data about Enam expression in western blots due to the lack of its antibody. These enamel matrix proteins were mainly secreted by ameloblasts during the presecretory and secretory stages. This was consistent with the result we observed in immunohistochemistry. This finding supported our speculation that Fam83h plays an important role in the presecretory and secretory stages of enamel formation. AMELX is the most abundant enamel matrix protein, and it could regulate crystal spacing in enamel formation. Some studies have suggested that ENAM plays a role in crystal elongation [36]. AMBN has been suggested to be a cell adhesion molecule that influences ameloblast growth and differentiation [37]. KLK4 helps remove the mass of previously secreted and partially hydrolysed matrix proteins in the maturation stage. A study showed that *KLK4* variation are associated with enamel hypomineralization [38]. Therefore, we speculated that Fam83h regulates the secretion of enamel matrix proteins such as Klk4 to affect crystal mineralization in the maturation stage and resulted in ADHCAI. Combining our findings with the data described above, we speculate that *Fam83h* may regulate the secretion of enamel matrix proteins in the presecretory and secretory stages and then affect ameloblast differentiation. However, the mechanisms by which *FAM83H* results in ADHCAI and plays a role in the maturation stage remain to be elucidated in future studies.

Conclusion

We investigated a case of five generations of a Chinese family diagnosed with AI and found a known nonsense variant (c.973 C > T) in exon 5 of the *FAM83H* gene that causes a truncated protein (p.R325X) in this Chinese family. Combining our findings with the data described above, Fam83h is highly expressed in presecretory and secretory ameloblasts and plays an important role during enamel formation. *FAM83H* regulates the secretion of enamel matrix proteins and affects ameloblast differentiation.

Supplementary Information The online version contains supplementary material available at https://doi.org/10.1007/s00784-022-04763-9.

Author contribution JZ and QD contributed to the study conception and design. Bioinformatics and statistical analyses were performed by LC and JY. Clinical data collection and analysis were performed by QM, XH, YY and QY. Material preparation, experiment, data collection and analyses performed by YX and MM. The first draft of the manuscript was written by YX and MM, and all authors commented on previous versions of the manuscript. All authors read and approved the final.

Funding We thank the patients and their family members for consenting to this research. This study was funded by grants from the National Natural Science Foundation of China (82170947) and the Applied Foundation in Science and Technology Office of Sichuan Province (2021YFG0230).

Declarations

Competing interests The authors declare no competing interests.

Ethical approval This study was approved by the Ethics Committee of the Sichuan Academy of Medical Sciences-Sichuan Provincial People's Hospital (Chengdu, China) [2020 (371)]. The animal experimental protocol was approved by the Ethics Committee of West China College of Stomatology, Sichuan University, Chengdu, China (WCHSIRB-D-2021–077).

Consent to participate Informed consent was obtained from the legal guardians of children involved in the study.

Conflict of interest The authors declare no competing interests.

References

1. Bartlett JD (2013) Dental enamel development: proteinases and their enamel matrix substrates. ISRN Dent 2013:684607. https://doi.org/10.1155/2013/684607
2. Lacruz RS, Habelitz S, Wright JT, Paine ML (2017) Dental enamel formation and inplications for oral health and disease. Physiol Rev 97(3):939–993. https://doi.org/10.1152/physrev.00030.2016
3. Sabandal MM, Schäfer E (2016) Amelogenesis imperfecta: review of diagnostic findings and treatment concepts. Odontology 104(3):245–256. https://doi.org/10.1007/s10266-016-0266-1
4. Simmer JP, Papagerakis P, Smith CE, Fisher DC, Rountrey AN, Zheng L, Hu JCC (2010) Regulation of dental enamel shape and

hardness. J Dent Res 89(10):1024–1038. https://doi.org/10.1177/0022034510375829
5. Smith CEL, Poulter JA, Antanaviciute A, Kirkham J, Brookes SJ, Inglehearn CF, Mighell AJ (2017) Amelogenesis imperfecta; genes, proteins and pathways. Front Physiol 8:435. https://doi.org/10.3389/fphys.2017.00435
6. Stephanopoulos G, Garefalaki ME, Lyroudia K (2005) Genes and related proteins involved in amelogenesis imperfecta. J Dent Res 84(12):1117–1126. https://doi.org/10.1177/154405910508401206
7. Lu Y, Papagerakis P, Yamakoshi Y, Hu JCC, Bartlett JD, Simmer JP (2008) Functions of KLK4 and MMP-20 in dental enamel formation. Biol Chem 389(6):695–700. https://doi.org/10.1515/BC.2008.080
8. Crawford PJM, Aldred M, Bloch-Zupan A (2007) Amelogenesis imperfecta. Orphanet J Rare Dis 2:17. https://doi.org/10.1186/1750-1172-2-17
9. Lee SK, Lee KE, Jeong TS, Hwang YH, Kim S, Hu JC, Simmer JP, Kim JW (2011) FAM83H mutations cause ADHCAI and alter intracellular protein localization. J Dent Res 90(3):377–381. https://doi.org/10.1177/0022034510389177
10. Zhang C, Song Y, Bian Z (2015) Ultrastructural analysis of the teeth affected by amelogenesis imperfecta resulting from FAM83H mutations and review of the literature. Oral Surgery Oral Medicine Oral Pathology Oral Radiology 119(2):E69–E76. https://doi.org/10.1016/j.oooo.2014.09.002
11. Hu JCC, Chun Y-HP, Al Hazzazzi T, Simmer JP (2007) Enamel formation and amelogenesis imperfecta. Cells Tissues Organs 186(1):78–85. https://doi.org/10.1159/000102683
12. Hyun HK, Lee SK, Lee KE, Kang HY, Kim EJ, Choung PH, Kim JW (2009) Identification of a novel FAM83H mutation and microhardness of an affected molar in autosomal dominant hypocalcified amelogenesis imperfecta. Int Endod J 42(11):1039–1043. https://doi.org/10.1111/j.1365-2591.2009.01617.x
13. Smith CEL, Whitehouse LLE, Poulter JA, Wilkinson Hewitt L, Nadat F, Jackson BR, Manfield IW, Edwards TA, Rodd HD, Inglehearn CF et al (2020) A missense variant in specificity protein 6 (SP6) is associated with amelogenesis imperfecta. Hum Mol Genet 29(9):1417–1425. https://doi.org/10.1093/hmg/ddaa041
14. Zheng Y, Lu T, Chen J, Li M, Xiong J, He F, Gan Z, Guo Y, Zhang L, Xiong F (2021) The gain-of-function FAM83H mutation caused hypocalcification amelogenesis imperfecta in a Chinese family. Clin Oral Investig 25(5):2915–2923. https://doi.org/10.1007/s00784-020-03609-6
15. Wang SK, Zhang H, Hu CY, Liu JF, Chadha S, Kim JW, Simmer JP, Hu JCC (2021) FAM83H and autosomal dominant hypocalcified amelogenesis imperfecta. J Dent Res 100(3):293–301. https://doi.org/10.1177/0022034520962731
16. Sriwattanapong K, Nitayavardhana I, Theerapanon T, Thaweesapphithak S, Chantarawaratit PO, Garuyakich R, Phokaew C, Porntaveetus T, Shotelersuk V (2021) Age-related dental phenotypes and tooth characteristics of FAM83H-associated hypocalcified amelogenesis imperfecta. Oral Dis. https://doi.org/10.1111/odi.13780
17. Kantaputra PN, Intachai W, Auychai P (2016) All enamel is not created equal: supports from a novel FAM83H mutation. Am J Med Genet A 170(1):273–276. https://doi.org/10.1002/ajmg.a.37406
18. Song YL, Wang CN, Zhang CZ, Yang K, Bian Z (2012) Molecular characterization of amelogenesis imperfecta in Chinese patients. Cells Tissues Organs 196(3):271–279. https://doi.org/10.1159/000334210
19. Wright JT, Torain M, Long K, Seow K, Crawford P, Aldred MJ, Hart PS, Hart TC (2011) Amelogenesis imperfecta: genotype-phenotype studies in 71 families. Cells Tissues Organs 194(2–4):279–283. https://doi.org/10.1159/000324339
20. Haubek D, Gjørup H, Jensen LG, Juncker I, Nyegaard M, Børglum AD, Poulsen S, Hertz JM (2011) Limited phenotypic variation of hypocalcified amelogenesis imperfecta in a Danish five-generation family with a novel FAM83H nonsense mutation. Int J Paediatr Dent 21(6):407–412. https://doi.org/10.1111/j.1365-263X.2011.01142.x
21. Chan HC, Estrella NM, Milkovich RN, Kim JW, Simmer JP, Hu JC (2011) Target gene analyses of 39 amelogenesis imperfecta kindreds. Eur J Oral Sci 119(Suppl 1):311–323. https://doi.org/10.1111/j.1600-0722.2011.00857.x
22. Ding Y, Estrella MRP, Hu YY, Chan HL, Zhang HD, Kim JW, Simmer JP, Hu JCC (2009) Fam83h is associated with intracellular vesicles and ADHCAI. J Dent Res 88(11):991–996. https://doi.org/10.1177/0022034509349454
23. Kim JW, Lee SK, Lee ZH, Park JC, Lee KE, Lee MH, Park JT, Seo BM, Hu JC, Simmer JP (2008) FAM83H mutations in families with autosomal-dominant hypocalcified amelogenesis imperfecta. Am J Hum Genet 82(2):489–494. https://doi.org/10.1016/j.ajhg.2007.09.020
24. Wang S-K, Hu Y, Yang J, Smith CE, Richardson AS, Yamakoshi Y, Lee Y-L, Seymen F, Koruyucu M, Gencay K et al (2016) Fam83h null mice support a neomorphic mechanism for human ADHCAI. Mol Genet Genomic Med 4(1):46–67. https://doi.org/10.1002/mgg3.178
25. Wang SK, Hu Y, Smith CE, Yang J, Zeng C, Kim JW, Hu JC, Simmer JP (2019) The enamel phenotype in homozygous Fam83h truncation mice. Mol Genet Genomic Med 7(6):e724. https://doi.org/10.1002/mgg3.724
26. Nasseri S, Nikkho B, Parsa S, Ebadifar A, Soleimani F, Rahimi K, Vahabzadeh Z, Khadem-Erfan MB, Rostamzadeh J, Baban B et al (2019) Generation of Fam83h knockout mice by CRISPR/Cas9-mediated gene engineering. J Cell Biochem 120(7):11033–11043. https://doi.org/10.1002/jcb.28381
27. Xin W, Wang W, Man Q, Zhao Y (2017) Novel FAM83H mutations in patients with amelogenesis imperfecta. Sci Rep 7:6075. https://doi.org/10.1038/s41598-017-05208-0
28. Du Q, Cao L, Liu Y, Pang C, Wu S, Zheng L, Jiang W, Na X, Yu J, Wang S et al (2021) Phenotype and molecular characterizations of a family with dentinogenesis imperfecta shields type II with a novel DSPP mutation. Ann Transl Med 9(22):1672. https://doi.org/10.21037/atm-21-5369
29. Kawano S, Morotomi T, Toyono T, Nakamura N, Uchida T, Ohishi M, Toyoshima K, Harada H (2002) Establishment of dental epithelial cell line (HAT-7) and the cell differentiation dependent on Notch signaling pathway. Connect Tissue Res 43(2–3):409–412. https://doi.org/10.1080/03008200290000637
30. Bäckman B, Holm AK (1986) Amelogenesis imperfecta: prevalence and incidence in a northern Swedish county. Community Dent Oral Epidemiol 14(1):43–47. https://doi.org/10.1111/j.1600-0528.1986.tb01493.x
31. Yu S, Quan J, Wang X, Sun X, Zhang X, Liu Y, Zhang C, Zheng S (2018) A novel FAM83H mutation in one Chinese family with autosomal-dominant hypocalcification amelogenesis imperfecta. Mutagenesis 33(4):333–340. https://doi.org/10.1093/mutage/gey019
32. Simmer JP, Richardson AS, Hu YY, Smith CE, Ching-Chun HuJ (2012) A post-classical theory of enamel biomineralization and why we need one. Int J Oral Sci 4(3):129–134. https://doi.org/10.1038/ijos.2012.59
33. Moradian-Oldak J (2012) Protein-mediated enamel mineralization Front Biosci (Landmark Ed) 17(6):1996–2023. https://doi.org/10.2741/4034

34. Kuga T, Kume H, Adachi J, Kawasaki N, Shimizu M, Hoshino I, Matsubara H, Saito Y, Nakayama Y, Tomonaga T (2016) Casein kinase 1 is recruited to nuclear speckles by FAM83H and SON. Sci Rep 6:34472. https://doi.org/10.1038/srep34472
35. Blackburn JB, D'Souza Z, Lupashin VV (2019) Maintaining order: COG complex controls Golgi trafficking, processing, and sorting. FEBS Lett 593(17):2466–2487. https://doi.org/10.1002/1873-3468.13570
36. Hu CC, Hart TC, Dupont BR, Chen JJ, Sun X, Qian Q, Zhang CH, Jiang H, Mattern VL, Wright JT et al (2000) Cloning human enamelin cDNA, chromosomal localization, and analysis of expression during tooth development. J Dent Res 79(4):912–919. https://doi.org/10.1177/00220345000790040501
37. Fukumoto S, Kiba T, Hall B, Iehara N, Nakamura T, Longenecker G, Krebsbach PH, Nanci A, Kulkarni AB, Yamada Y (2004) Ameloblastin is a cell adhesion molecule required for maintaining the differentiation state of ameloblasts. J Cell Biol 167(5):973–983. https://doi.org/10.1083/jcb.200409077
38. Smith CEL, Kirkham J, Day PF, Soldani F, McDerra EJ, Poulter JA, Inglehearn CF, Mighell AJ, Brookes SJ (2017) A fourth KLK4 mutation is associated with enamel hypomineralisation and structural abnormalities. Front Physiol 29(8):333. https://doi.org/10.3389/fphys.2017.00333

Publisher's note Springer Nature remains neutral with regard to jurisdictional claims in published maps and institutional affiliations.

Springer Nature or its licensor (e.g. a society or other partner) holds exclusive rights to this article under a publishing agreement with the author(s) or other rightsholder(s); author self-archiving of the accepted manuscript version of this article is solely governed by the terms of such publishing agreement and applicable law.